US006961123B1

(12) **United States Patent**
Wang et al.

(10) **Patent No.: US 6,961,123 B1**
(45) **Date of Patent: Nov. 1, 2005**

(54) METHOD AND APPARATUS FOR OBTAINING INFORMATION FROM POLARIZATION-SENSITIVE OPTICAL COHERENCE TOMOGRAPHY

(75) Inventors: **Lihong Wang**, College Station, TX (US); **Shuliang Jiao**, College Station, TX (US)

(73) Assignee: **The Texas A&M University System**, College Station, TX (US)

(*) Notice: Subject to any disclaimer, the term of this patent is extended or adjusted under 35 U.S.C. 154(b) by 124 days.

(21) Appl. No.: **10/260,236**

(22) Filed: **Sep. 27, 2002**

Related U.S. Application Data

(60) Provisional application No. 60/325,990, filed on Sep. 28, 2001.

(51) **Int. Cl.**^{7} **G01J 4/00**
(52) **U.S. Cl.** **356/364**
(58) **Field of Search** 356/364–369; 250/225, 227.17

(56) **References Cited**

U.S. PATENT DOCUMENTS

6,043,887 A	*	3/2000	Allard et al.	356/364
6,208,415 B1	*	3/2001	De Boer et al.	356/450
6,504,604 B1	*	1/2003	Holland	356/73.1
6,538,738 B1	*	3/2003	Okamoto	356/364
2002/0113972 A1	*	8/2002	Rosenfeldt et al.	356/477
2004/0036886 A1	*	2/2004	Motamedi et al.	356/477

OTHER PUBLICATIONS

Jose J. Gil and Eusebio Bernabeu, "*Obtainment of the polarizing and retardation parameters of a non–depolarizing optical system from the polar decomposition of its Mueller matrix*," Optik 76, No. 2, pp. 67–71, 1987.

N. Vansteenkiste, P. Vignolo, and A. Aspect, "*Optical reversibility theoems for polarization: application to remote control of polarization*," © 1993 Optical Society of America, J. Opt. Soc. Am. A, vol. 10, No. 10, pp. 2240–2245, Oct. 1993.

F. Le Roy–Brehonnet and B. Le Jeune, "*Utilization of Mueller Matrix Formalism to Obtain Optical Targets Depolarization and Polarization Properties*," © 1997 Elsevier Science Ltd., Prog. Quant. Electr. vol. 21, No. 2, pp. 109–151, 1997.

Johannes F. de Boer, Thomas E. Milner, Martin J.C. van Gemert, and J. Stuart Nelson, "*Two–dimensional birefringence imaging in biological tissue by polarization–sensitive optical coherence tomography*," © 1997 Optical Society of America, Optics Letters, vol. 22, No. 12, pp. 934–936, Jun. 15, 1997.

M. J. Everett, K. Schoenenberger, B. W. Colston, Jr., and L. B. Da Silva, *Birefringence characterization of biological tissue by use of optical coherence tomography*, © 1998 Optical Society of America, Optics Letters, vol. 23, No. 3, pp. 228–230, Feb. 1, 1998.

Johannes F. de Boer, Shyam M. Srinivas, Arash Malekafzali, Zhongping Chen, and J. Stuart Nelson, "*Imaging thermally damaged tissue by polarization sensitive optical coherence tomography*," © 1998 OSA, Optics Express, vol. 3, No. 6, pp. 212–218, Sep. 14, 1998.

(Continued)

Primary Examiner—Michael P. Stafira
(74) *Attorney, Agent, or Firm*—Baker Botts L.L.P.

(57) ABSTRACT

An apparatus includes a first section operable to detect polarization-sensitive radiation emitted by an object, and a second section operable to determine a Jones matrix based on information obtained by the first section from the polarization-sensitive radiation. The second section thereafter transforms the Jones matrix into a Mueller matrix, the Mueller matrix being representative of properties of the object.

27 Claims, 7 Drawing Sheets

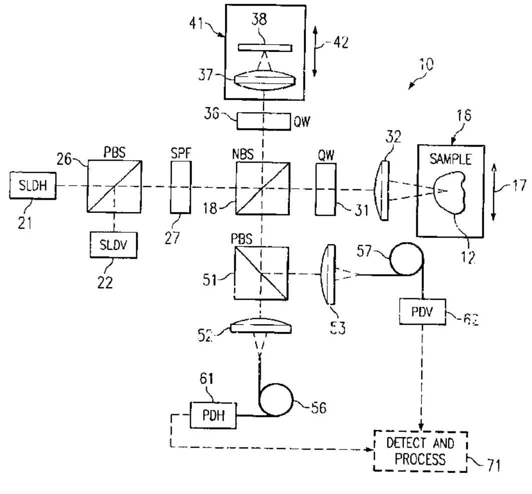

OTHER PUBLICATIONS

Johannes F. de Boer, Thomas E. Milner, and J. Stuart Nelson, "*Determination of the depth–resolved Stokes parameters of light backscattered from turbid media by use of polarization–sensitive optical coherence tomography*," © 1999 Optical Society of America, Optics Letters, vol. 24, No. 5, pp. 300–302, Mar. 1, 1999.

Gang Yao and Lihong V. Wang, "*Two–dimensional depth–resolved Mueller matrix characterization of biological tissue by optical coherence tomography*," © 1999 Optical Society of America, Optics Letters, vol. 24, No. 8, pp. 537–539, Apr. 15, 1999.

Yonghua Zhao, Zhongping Chen, Christopher Saxer, Shaohua Xiang, Johannes F. de Boer, and J. Stuart Nelson, "*Phase–resolved optical coherence tomography and optical Doppler tomography for imaging blood flow in human skin with fast scanning speed and high velocity sensitivity*," © 2000 Optical Society of America, Optics Letters, vol. 25, No. 2, pp. 114–116, Jan. 15, 2000.

Shuliang Jiao, Gang Yao, and Lihong V. Wang, "*Depth–resolved two–dimensional Stokes vectors of backscattered light and Mueller matrices of biological tissue measured with optical coherence tomography*," © 2000 Optical Society of America, Applied Optics, vol. 39, No. 34, pp. 6318–6324, Dec. 1, 2000.

* cited by examiner

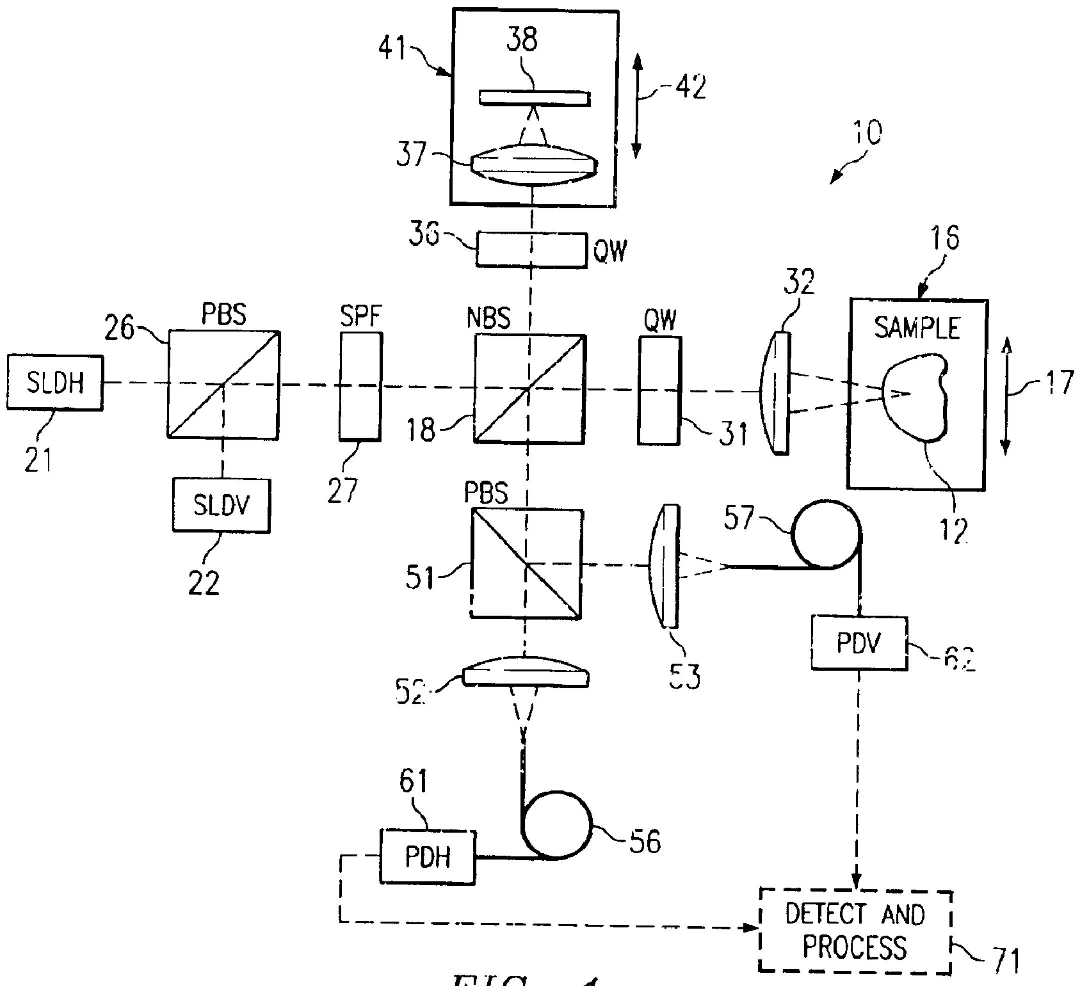
41
38
42
37
10
36
QW
16
32
PBS
SPF
NBS
QW
26
SAMPLE
SLDH
17
18
31
21
SLDV
27
12
PBS
57
51
22
PDV
62
52
53
61
56
PDH
DETECT AND
PROCESS
71

FIG. 1

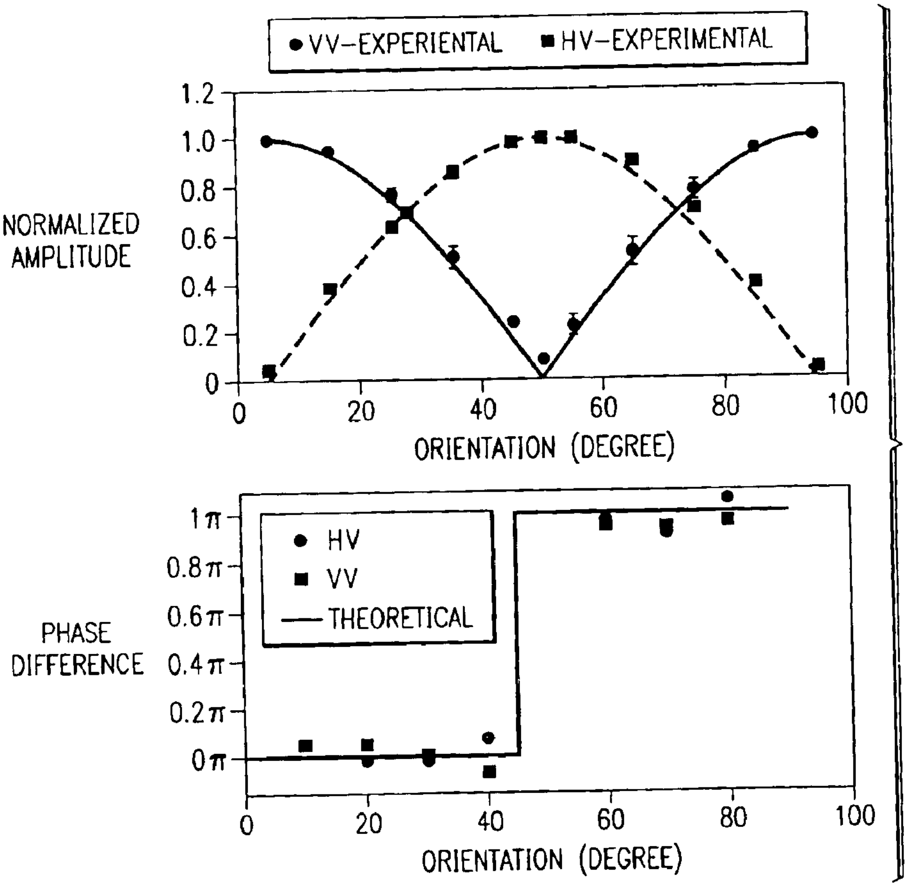
● VV-EXPERIENTAL
■ HV-EXPERIMENTAL
NORMALIZED AMPLITUDE
1.2
1.0
0.8
0.6
0.4
0.2
0
0
20
40
60
80
100
ORIENTATION (DEGREE)
PHASE DIFFERENCE
1π
0.8π
0.6π
0.4π
0.2π
0π
● HV
■ VV
— THEORETICAL
0
20
40
60
80
100
ORIENTATION (DEGREE)

FIG. 2

FIG. 3

FIG. 4

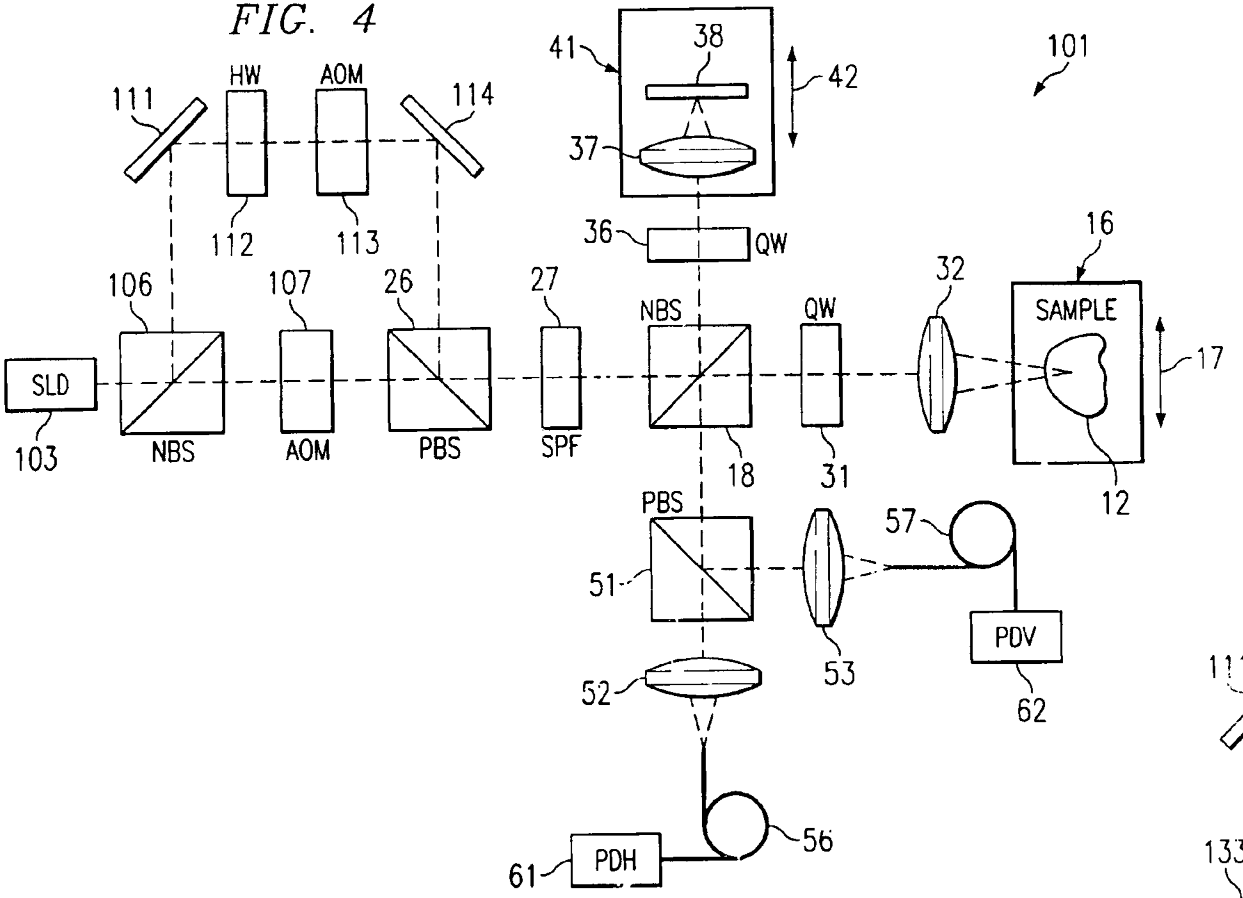
101
41
38
42
37
36
QW
111
HW
AOM
114
112
113
106
107
26
27
NBS
QW
32
16
SAMPLE
17
SLD
103
NBS
AOM
PBS
SPF
18
31
12
PBS
57
51
PDV
53
62
52
56
PDH
61

FIG. 5

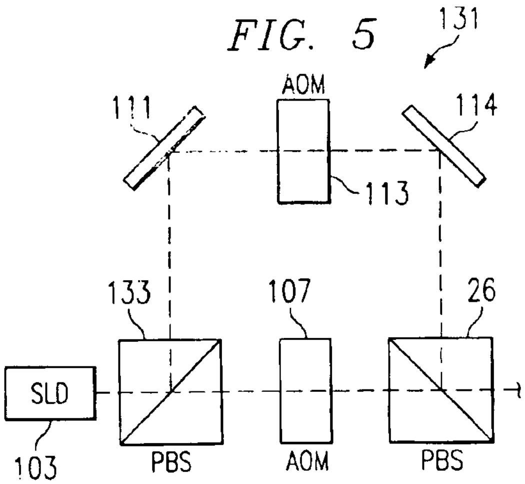
131
AOM
111
114
113
133
107
26
SLD
103
PBS
AOM
PBS

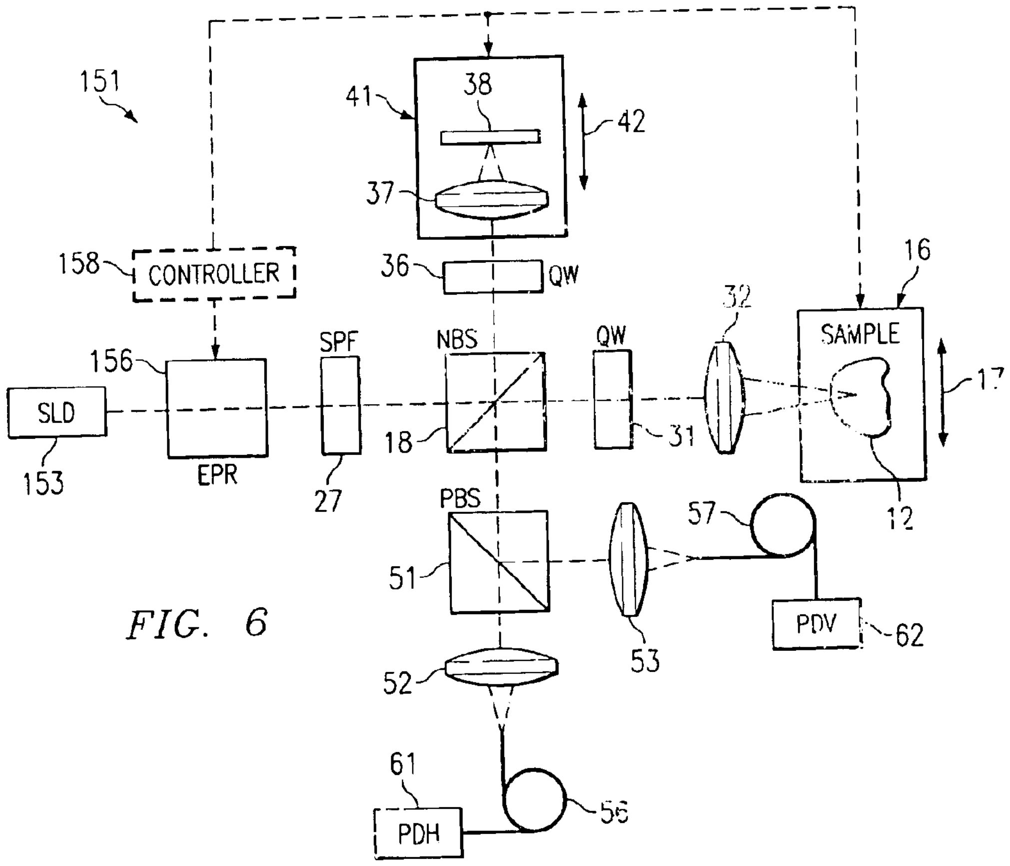
151
41
38
42
37
158
CONTROLLER
36
QW
16
32
SAMPLE
156
SPF
NBS
QW
SLD
17
18
31
153
EPR
27
12
PBS
57
51
PDV
62
52
53
61
56
PDH

FIG. 6

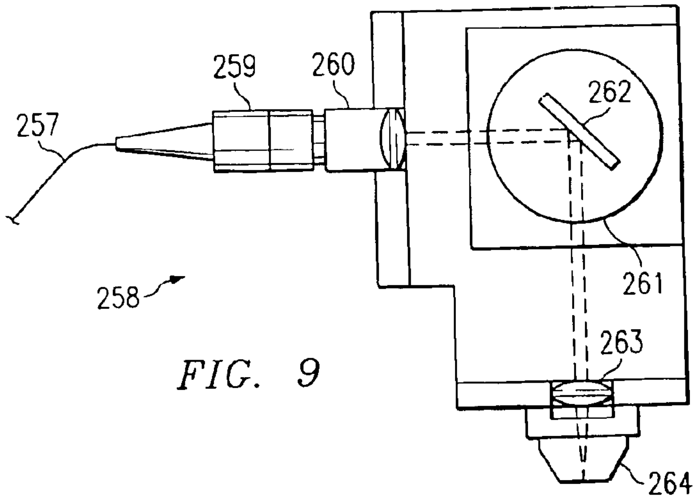
259
260
262
257
261
258
263
264

FIG. 9

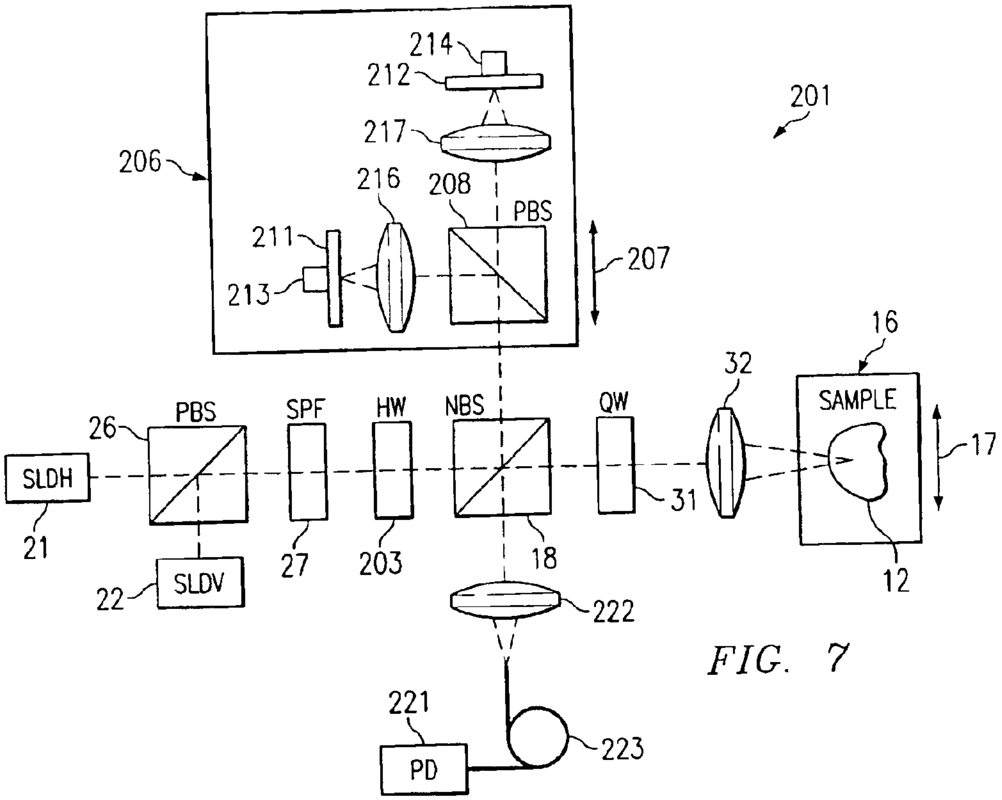

FIG. 7

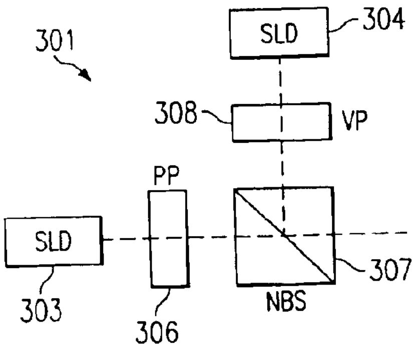

FIG. 10

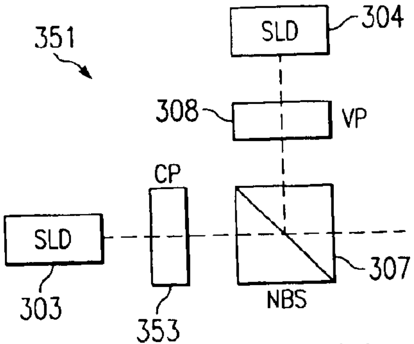

FIG. 11

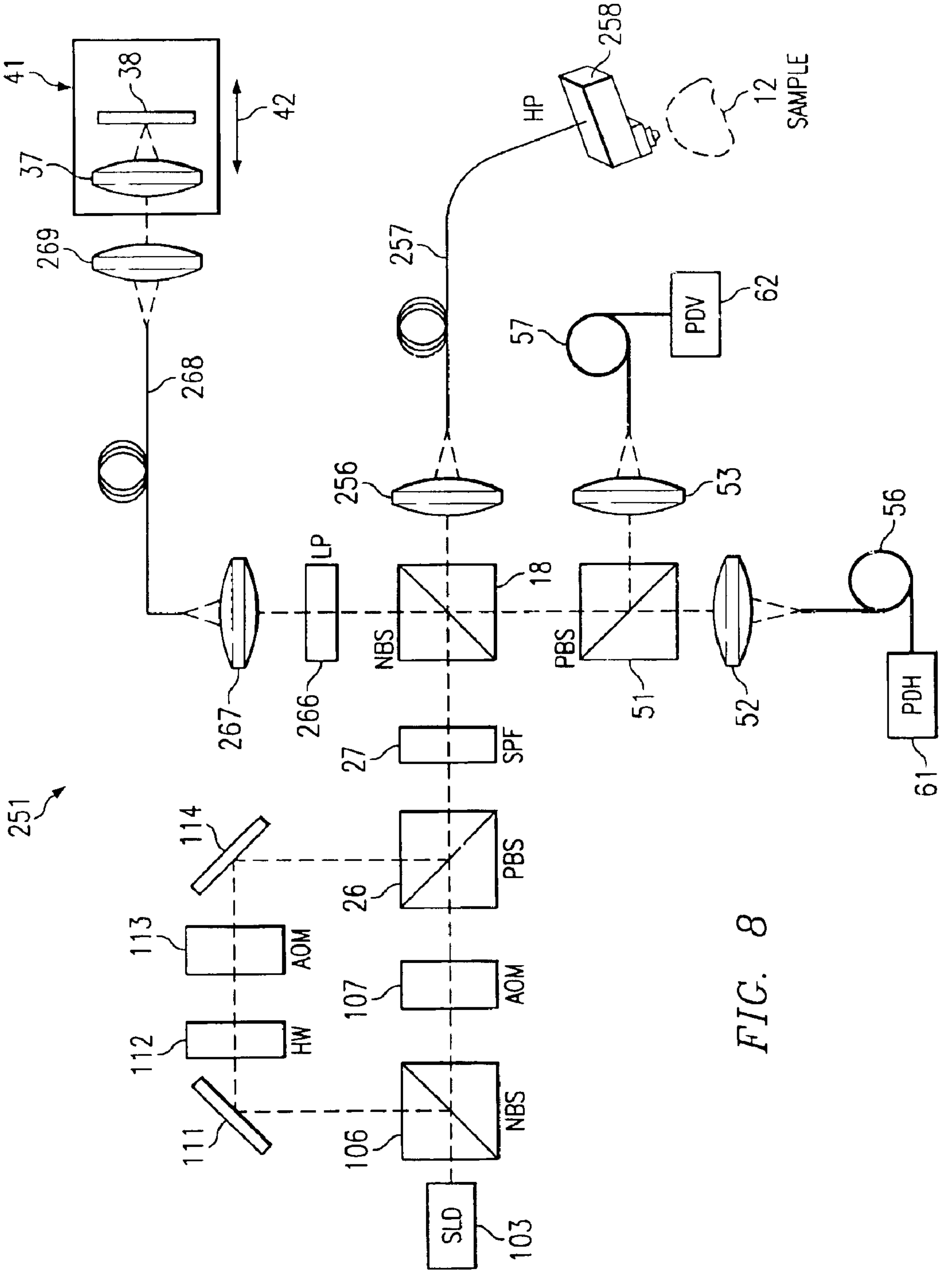
251
SLD
103
NBS
106
111
112
HW
113
AOM
107
AOM
114
PBS
26
27
SPF
267
266
LP
NBS
18
PBS
51
52
PDH
61
56
256
53
57
PDV
62
268
269
37
38
41
42
257
HP
258
12
SAMPLE

FIG. 8

METHOD AND APPARATUS FOR OBTAINING INFORMATION FROM POLARIZATION-SENSITIVE OPTICAL COHERENCE TOMOGRAPHY

This application claims the priority under 35 U.S.C. §119 of provisional application No. 60/325,990 filed Sep. 28, 2001.

GOVERNMENT RIGHTS

This invention was made with government support under Contract Nos. R21 RR15368 and R01 CA71980 awarded by the National Institutes of Health, and by National Science Foundation grant BES-9734491. The government has certain rights in this invention.

TECHNICAL FIELD OF THE INVENTION

The present invention relates generally to techniques for analyzing radiation and, more particularly, to techniques for obtaining information from polarization-sensitive radiation.

BACKGROUND OF THE INVENTION

It is known that one good way to ascertain the optical polarization properties of an object or sample is to determine its Mueller matrix. By using polarimetry in combination with optical coherence tomography (OCT), the Mueller matrix of a sample can be acquired with OCT resolution. The degree of polarization (DOP) of the back-scattered light measured with OCT remains unity throughout the detection range, indicating that the measured Mueller matrix is non-depolarizing.

However, existing techniques for measuring the Mueller matrix of a sample are relatively time consuming. As a practical matter, the relatively time-consuming nature of these existing techniques effectively limits their use to stable samples, such as bones. These existing techniques are generally not suitable for measuring the Mueller matrix of an unstable sample, such as soft tissue. For an unstable sample such as biological tissue, it would typically be necessary to determine the Mueller matrix during a single scan of the type known in the art as an A scan, and existing systems are not sufficiently fast to do this.

SUMMARY OF THE INVENTION

One form of the present invention involves: causing an object to emit polarization-sensitive radiation; detecting the polarization-sensitive radiation; determining a Jones matrix based on information obtained in the detecting step from the polarization-sensitive radiation; and transforming the Jones matrix into a Mueller matrix, the Mueller matrix being representative of properties of the object.

BRIEF DESCRIPTION OF THE DRAWINGS

A better understanding of the present invention will be realized from the detailed description which follows, taken in combination with the accompanying drawings, in which:

FIG. **1** is a block diagram of a polarization-sensitive optical coherence tomography (OCT) apparatus, which embodies aspects of the present invention;

FIG. **2** includes two related graphs which are respectively presented in the upper and lower portions thereof;

FIG. **3** is a diagrammatic view of an array of Mueller matrix images obtained using techniques according to the present invention;

FIG. **4** is a block diagram of an apparatus which is an alternative embodiment of the apparatus of FIG. **1**;

FIG. **5** is a block diagram of an apparatus which is an alternative embodiment of a portion of the apparatus of FIG. **4**;

FIG. **6** is a block diagram of an apparatus which is yet another alternative embodiment of the apparatus of FIG. **1**;

FIG. **7** is a block diagram of an apparatus which is still another alternative embodiment of the apparatus of FIG. **1**;

FIG. **8** is a block diagram of an apparatus which is another alternative embodiment of the apparatus of FIG. **4**;

FIG. **9** is a diagrammatic sectional side view of a hand-held probe which is a component of the apparatus of FIG. **8**;

FIG. **10** is a block diagram of an apparatus which is an alternative embodiment of part of the apparatus of FIG. **1**; and

FIG. **11** is a block diagram of an apparatus which is an alternative embodiment of the apparatus of FIG. **10**.

DETAILED DESCRIPTION

FIG. **1** is a block diagram of a polarization-sensitive optical coherence tomography (OCT) apparatus **10**, which embodies aspects of the present invention. As discussed in more detail later, the apparatus **10** uses polarization-sensitive OCT to optically and non-destructively collect information about a sample **12**. The sample **12** is not itself a part of the apparatus **10**, and may be biological tissue, such as cartilage, collagen, or a retina. Alternatively, the sample **12** could be a non-biological material, such as a piece of a polymer material. Through the use of polarization properties as a contrast mechanism, polarization-sensitive OCT can reveal some information about biological tissue or other material that is not available with conventional OCT techniques.

The apparatus **10** includes a translation stage in the form of a table **16**, which has the sample **12** supported thereon, and which is supported for reciprocal linear movement in directions indicated by a double-headed arrow **17**. Movement of the table **16** permits a linear lateral scan of the sample **12**. The apparatus **10** further includes a non-polarizing beam splitter **18**, which is disposed functionally at the center of the apparatus **10**. The portion of the apparatus to the left of the splitter **18** is referred to as the source arm, the portion above the splitter **18** is referred to as the reference arm, the portion to the right of the splitter **18** is referred to as the sample arm, and the portion below the splitter **18** is referred to as the detection arm.

The source arm to the left of the splitter **18** includes two superluminescent diodes **21** and **22**, which each serve as a low-coherence light source having a central wavelength of approximately 850 nm, and a full width at half maximum (FWHM) bandwidth of 26 nm. The diodes **21** and **22** are respectively modulated at 3 KHz and 3.5 KHz. The two source beams from the diodes **21** and **22** travel to and are merged by a polarizing beam splitter **26**. The composite optical signal travels to and is filtered by a spatial filter assembly **27**, and then travels to a non-polarizing beam splitter **18**.

The beam from the diode **21** is split into two components by the splitter **18**, one of which travels upwardly into the reference arm, and the other of which travels rightwardly into the sample arm. Similarly, the beam from the diode **22** is split into two components by the splitter **18**, and these two components respectively travel upwardly into the reference arm and rightwardly into the sample arm.

The sample arm to the right of the splitter **18** includes a quarter wave plate, the fast axis of which is oriented at 45°. The sample arm also includes an objective lens 32, with f=15 mm and NA=0.15. Radiation from the splitter **18** passes through the plate **31** and is focused by the lens **32** onto the sample **12**. A portion of this radiation is reflected, and travels back through the lens **32** and plate **31** to the splitter **18**.

The reference arm above the splitter **18** includes a quarter wave plate **36**, a lens **37**, and a mirror **38**. The lens **37** and mirror **38** are supported on a table **41**, which in turn is supported for reciprocal linear movement in directions indicated by a double-headed arrow **42**. A not-illustrated mechanism moves the table **41** reciprocally for depth scan, and generates a carrier frequency of approximately 1.2 KHz.

As mentioned above, the splitter **18** directs two beam components into the reference arm, and these beam components travel upward through the plate **36**, and are focused by the lens **37** onto the mirror **38**. Substantially all of this radiation is reflected by the mirror **38**, and travels back through the lens **37** and plate **36** to the splitter **18**. The fast axis of the plate **36** is oriented at 22.5°. Consequently, after these components pass through the plate **36** twice, the component representing horizontal polarization is converted into 45° polarization, while the component representing vertical polarization is converted into −45° polarization.

The components reflected by the sample **12** and the components reflected by the mirror **38** arrive back at the splitter **18**, and are combined by the splitter **18**. This combined light beam travels downwardly from the splitter **18** into the detector arm, where it is split into two orthogonal polarization components by a polarizing beam splitter **51**. These two components each pass through a respective objective lens **52** or **53**, and are each coupled into a respective single-mode optical fiber **56** or **57**. At the opposite end of each of the fibers **56** and **57** is a respective photodiode **61** or **62**. The photodiode **61** detects the horizontal component of the radiation, and the photodiode **62** detects the vertical component of the radiation. The outputs of the photodiodes **61** and **62** are each coupled to a circuit **71** which has a portion that serves as a data acquisition system, the circuit **71** detecting and processing the information produced by the diodes **61** and **62**. In the disclosed embodiment, the circuit **71** digitizes the output of each diode in a known manner at a sampling rate of about 50,000 samples per second.

Turning now to the issue of how the data collected by the circuit 71 is analyzed, it is known in the art that one good way to ascertain the optical polarization properties of an object or sample is to determine its Mueller matrix. By using polarimetry in combination with OCT, the Mueller matrix of a sample can be acquired with OCT resolution. However, existing techniques for measuring the Mueller matrix of a sample are relatively time consuming. As a practical matter, the relatively time-consuming nature of these existing techniques effectively limits their use to stable samples, such as bones. These existing techniques are generally not suitable for measuring the Mueller matrix of an unstable sample, such as soft tissue. In particular, for an unstable sample such as biological tissue, it would be necessary to determine the Mueller matrix during a single scan of the type known in the art as an A scan, and existing systems were not sufficiently fast to do this.

According to one feature of the present invention, a different approach is taken. In particular, the depth-resolved 2×2 Jones matrix J of a sample is acquired during a single A scan, in a manner discussed in more detail later. The 2×2 Jones matrix J is then transformed into an equivalent 4×4 Mueller matrix.

In more detail, a Mueller matrix is suitable for all kinds of optical systems, but a Jones matrix can only be applied to a non-depolarizing optical system. In a non-depolarizing optical system, a Jones matrix can completely characterize the polarization properties of the optical system. In other words, for a non-depolarizing optical system, a Jones matrix is equivalent to a Mueller matrix. An aspect of the present invention relates to experimental proof that the degree of polarization (DOP) of back-scattered light measured with OCT remains unity throughout the detection range, indicating that the measured Mueller matrix is non-depolarizing. This in turn means that an equivalent Jones matrix can be used instead of the Mueller matrix.

A Jones matrix is a 2×2 matrix based on complex numbers, whereas a Mueller matrix is a 4×4 matrix based on real numbers. A Jones matrix has four complex elements, in which one phase is arbitrary. Consequently, seven real parameters are independent. Equivalently, there are seven independent parameters in a non-depolarizing Mueller matrix.

A Jones matrix (J) transforms an input Jones vector (E_{IN}) into an output Jones vector (E_{OUT}), while a Mueller matrix (M) transforms an input Stokes vector (S_{IN}) into an output Stokes vector (S_{OUT}):

$$E_{OUT} = \begin{bmatrix} E_{OH} \\ E_{OV} \end{bmatrix} = JE_{IN} = \begin{bmatrix} J_{11} & J_{12} \\ J_{21} & J_{22} \end{bmatrix} \begin{bmatrix} E_{iH} \\ E_{iV} \end{bmatrix}, \tag{1}$$

$$S_{OUT} = \begin{bmatrix} S_0 \\ S_1 \\ S_2 \\ S_3 \end{bmatrix} = MS_{IN} = \begin{bmatrix} M_{00} & M_{01} & M_{02} & M_{03} \\ M_{10} & M_{11} & M_{12} & M_{13} \\ M_{20} & M_{21} & M_{22} & M_{23} \\ M_{30} & M_{31} & M_{32} & M_{33} \end{bmatrix} \begin{bmatrix} S_{i0} \\ S_{i1} \\ S_{i2} \\ S_{i3} \end{bmatrix}, \tag{2}$$

where E_{OH} and E_{OV} are the horizontal and vertical components of the electric vector of the output light field; E_{iH} and E_{iV} are the horizontal and vertical components of the electric vector of the input light field; S_0, S_1, S_2 and S_3 are the elements of the Stokes vector of the output light; and S_{i0}, S_{i1}, S_{i2} and S_{i3} are the elements of the Stokes vector of the input light, respectively.

The Jones matrices of a homogenous partial polarizer (J_P) and a homogenous elliptical retarder (J_R) can be expressed as

$$J_P = \begin{bmatrix} P_1\cos^2\alpha + P_2\sin^2\alpha & (P_1 - P_2)\sin\alpha\cos\alpha e^{-i\Delta} \\ (P_1 - P_2)\sin\alpha\cos\alpha e^{i\Delta} & P_1\sin^2\alpha + P_2\cos^2\alpha \end{bmatrix}, \tag{3}$$

$$J_R = \begin{bmatrix} e^{i\varphi/2}\cos^2\theta + e^{-i\varphi/2}\sin^2\theta & (e^{i\varphi/2} - e^{-i\varphi/2})\sin\theta\cos\theta e^{-i\delta} \\ (e^{i\varphi/2} - e^{-i\varphi/2})\sin\theta\cos\theta e^{-i\delta} & e^{i\varphi/2}\sin^2\theta + e^{-i\varphi/2}\cos^2\theta \end{bmatrix},$$

where P_1, P_2 are the principal coefficients of the amplitude transmission for the two orthogonal polarization eigenstates; α is the orientation of J_P; ϕ and θ are the retardation and orientation of J_R; and Δ and δ are the phase differences for the vertical and horizontal components of the eigenstates of J_P and J_R, respectively. A retarder is called elliptical when its eigenvectors are those of elliptical polarization states. A polarizing element is called homogeneous when the two eigenvectors of its Jones matrix are orthogonal. The Jones-matrix of a non-depolarizing optical system can be transformed into an equivalent non-depolarizing Mueller matrix by the following relationship:

$$\begin{aligned} M &= U(J \otimes J^*)U^{-1} \\ &= U\begin{bmatrix} J_{11}J^* & J_{12}J^* \\ J_{21}J^* & J_{22}J^* \end{bmatrix}U^{-1} \\ &= U\begin{bmatrix} J_{11}J_{11}^* & J_{11}J_{12}^* & J_{12}J_{11}^* & J_{12}J_{12}^* \\ J_{11}J_{21}^* & J_{11}J_{22}^* & J_{12}J_{21}^* & J_{12}J_{22}^* \\ J_{21}J_{11}^* & J_{21}J_{12}^* & J_{22}J_{11}^* & J_{22}J_{12}^* \\ J_{21}J_{21}^* & J_{21}J_{22}^* & J_{22}J_{21}^* & J_{22}J_{22}^* \end{bmatrix}U^{-1}; \end{aligned} \tag{4A}$$

and a Jones vector of a light field can be transformed into a Stokes vector by

$$\begin{aligned} S = \sqrt{2}\,U(E \otimes E^*) &= \sqrt{2}\,U\begin{bmatrix} E_H E^* \\ E_V E^* \end{bmatrix} \\ &= \sqrt{2}\,U\begin{bmatrix} E_H E_H^* \\ E_H E_V^* \\ E_V E_H^* \\ E_V E_V^* \end{bmatrix}, \end{aligned} \tag{4B}$$

where ⊗ represents the Kronecker tensor product and U is the 4×4 Jones-Mueller transformation matrix:

$$U = \frac{1}{\sqrt{2}}\begin{bmatrix} 1 & 0 & 0 & 1 \\ 1 & 0 & 0 & -1 \\ 0 & 1 & 1 & 0 \\ 0 & i & -i & 0 \end{bmatrix}.$$

At least two independent incident polarization states, which are not necessarily orthogonal, are needed to fully determine a Jones matrix.

As mentioned above, the portions of the apparatus **10** of FIG. **1** which are above and to the right of the splitter **18** are respectively referred to as the reference arm and the sample arm. For OCT signals based on single-backscattered photons, the incident Jones vector E_i to the sample arm is transformed to the detected Jones vector E_0 by

$$\begin{aligned} E_o &= J_{NBS}J_{QB}J_{SB}J_M J_{SI}J_{QI}E_i \\ &= J_{NBS}J_{QB}JJ_{QI}E_i = J_T E_i \end{aligned} \tag{5}$$

where J_{QI} and J_{QB} are the Jones matrices of a quarter wave plate for the incident and backscattered light, respectively; J_{SI} and J_{SB} are the Jones matrices of the sample for the incident and backscattered light, respectively; J_M is the Jones matrix of the single backscatterer (the same Jones matrix as for a mirror); J_{NBS} is the Jones matrix of the reflecting surface of the non-polarizing beam splitter; J is the combined round-trip Jones matrix of the scattering medium; and J_T is the overall round-trip Jones matrix.

In Equation (5), the output Jones vector E_0 is constructed for each light source from the measured horizontal and vertical components of the OCT signal. Upon acquiring the output Jones vectors, and knowing the input Jones vectors, the overall round-trip Jones matrix J_T can be calculated. The Jones matrix J of the sample can be extracted from J_T by eliminating the effect of the Jones matrices of the quarter wave plate, the mirror and the beam splitter. As a necessary condition, the two light sources must be independent of each other, which means that there is an arbitrary phase difference between the two measured Jones vectors for the two light sources. The arbitrary phase difference must be eliminated in order to calculate J_T.

In the commonly used convention, J_M transforms the polarization state of the forward light expressed in the forward coordinate system into the polarization state expressed in the backward coordinate system. Similarly, J_{NBS} transforms the polarization state of the backward light into the polarization state expressed in the detection coordinate system. However, the polarization states of both the forward and backward light are expressed here in the forward coordinate system. In this convention, J_M and J_{NBS} are unitary:

$$J_M = J_{NBS} = \begin{bmatrix} 1 & 0 \\ 0 & 1 \end{bmatrix}.$$

In each A-scan, the optical paths for the forward and backward light are the same, and therefore the Jones' reversibility theorem can be applied. The Jones reversibility theorem indicates that the Jones matrices J_{BWD} and J_{FWD} of an ordinary optical element for the backward and forward light propagations have the following relationship if the same coordinate system is used for the Jones vectors: $J_{BWD}=J_{FWD}{}^T$. Therefore, the following relationships apply:

$$J_{SB} = J_{SI}^T,\ J_{QB} = J_{QI}^T = \frac{1}{\sqrt{2}}\begin{bmatrix} 1 & i \\ i & 1 \end{bmatrix},$$

$$J=J_{SB}J_MJ_{SI}=J_{SI}{}^TJ_{SI}=J^T,$$

$$J_T=J_{NBS}J_{QB}JJ_{QI}=J_{QI}{}^TJJ_{QI}=J_T{}^T.$$

In other words, matrices J and J_T are transpose symmetric. This property of transpose symmetry is significant in regard to eliminating the arbitrary phase difference between the two light sources. Because of this symmetry, the number of independent parameters in the Jones matrix is further reduced from seven to five.

For the multiply scattered photons, Equation (5) still holds if the probabilities for photons to travel along the same round-trip path but in opposite directions are equal, which is a valid assumption when the source and detector have reciprocal characteristics. Because these photons are coherent, the round-trip Jones matrix of the sample J is the sum of the Jones matrices of all the possible round-trip paths; and for each possible path—for example, the k-th path—the round-trip Jones matrix is the sum of the Jones matrices for the two opposite directions [J_i(k) and J_r(k)]. Consequently, it follows that:

$$J = \sum_k [J_i(k) + J_r(k)] = \sum_k \{J_i(k) + [J_i(k)]^T\} = J^T.$$

In other words, J as well as J_T still possesses the transpose symmetry even if multiple scattering occurs, so long as the source and the detector meet the condition.

After calculation, Equation (5) can be expressed as

$$\begin{aligned} \begin{bmatrix} E_{oH} \\ E_{oV} \end{bmatrix} &= \begin{bmatrix} \frac{i}{2}(J_{11} - 2iJ_{12} - J_{22}) & \frac{1}{2}(J_{11} + J_{22}) \\ \frac{1}{2}(J_{11} + J_{22}) & \frac{i}{2}(-J_{11} - 2iJ_{12} + J_{22}) \end{bmatrix} \times \begin{bmatrix} E_{iH} \\ E_{iV} \end{bmatrix} \\ &= \begin{bmatrix} J_{T11} & J_{T12} \\ J_{T12} & J_{T22} \end{bmatrix} \times \begin{bmatrix} E_{iH} \\ E_{iV} \end{bmatrix}, \end{aligned} \tag{6A}$$

where J_{ij} and J_{Tij}(i,j=1,2) are the elements of J and J_T, respectively. For two light sources of independent polarization states, Equation (6A) can be rearranged as

$$\begin{bmatrix} E_{oH1} & E_{oH2} \\ E_{oV1} & E_{oV2} \end{bmatrix} = \begin{bmatrix} J_{T11} & J_{T12} \\ J_{T12} & J_{T22} \end{bmatrix} \times \begin{bmatrix} E_{iH1} & E_{iH2}e^{i\beta} \\ E_{iV1} & E_{iV2}e^{i\beta} \end{bmatrix}, \tag{6B}$$

where E_{oH1} and E_{oH2}, E_{oV1} and E_{oV2} are the elements of the Jones vectors of source **1** and source **2**, respectively; and β is the random initial phase-difference between the two light sources due to the mutual independence of them. J_T can be calculated from Equation (6B) as

$$\begin{aligned} \begin{bmatrix} J_{T11} & J_{T12} \\ J_{T12} & J_{T22} \end{bmatrix} &= \begin{bmatrix} E_{oH1} & E_{oH2} \\ E_{oV1} & E_{oV2} \end{bmatrix} \times \begin{bmatrix} E_{iH1} & E_{iH2}e^{i\beta} \\ E_{iV1} & E_{iV2}e^{i\beta} \end{bmatrix}^{-1} \\ &= \frac{1}{D}\begin{bmatrix} E_{oH1} & E_{oH2} \\ E_{oV1} & E_{oV2} \end{bmatrix} \times \begin{bmatrix} E_{iV2}e^{i\beta} & -E_{iH2}e^{i\beta} \\ -E_{iV1} & E_{iH1} \end{bmatrix}, \end{aligned} \tag{6C}$$

so long as the determinant

$$D = \begin{vmatrix} E_{iH1} & E_{iH2}e^{i\beta} \\ E_{iV1} & E_{iV2}e^{i\beta} \end{vmatrix} = e^{i\beta}\begin{vmatrix} E_{iH1} & E_{iH2} \\ E_{iV1} & E_{iV2} \end{vmatrix} \neq 0,$$

or in other words, the two light sources are not in the same polarization state. The random phase difference β can be eliminated with the transpose symmetry of J_T.

$$e^{\beta}(E_{oH1}E_{iH2}+E_{oV1}EiV2)=(E_{ov2}E_{iV1}+E_{oH2}E_{ih1}). \tag{6D}$$

Equation (6D) can solved when $(E_{oH1}E_{iH2}+E_{oV1}E_{iV2})\neq 0$. Once J_T is found, J can then be determined from J_T. Six real parameters of J can be calculated, in which one phase is arbitrary and can be subtracted from each element, and eventually five independent parameters are retained.

When $(E_{oH1}E_{iH2}+E_{oV1}E_{iV2})=0$, it is not possible to eliminate the random phase by using the transpose symmetry. This situation happens if, aside from producing a mirror reflection, the sample arm does not alter the polarization states of the two incident beams. For example, this situation occurs if (1) a horizontal or vertical incident beam is used, (2) a quarter wave plate is not inserted in the sample arm, and (3) the fast axis of a birefringent sample is horizontal or vertical. The use of the quarter wave plate at a 45° orientation in the sample arm can ameliorate the situation. However, there are still some drawbacks with this configuration. For example, when the round-trip Jones matrix J is equivalent to that of a half wave plate with its fast axis oriented at 45°, and thus J_T is equivalent to a unitary matrix, then $(E_{oH1}E_{iH2}+E_{oV1}E_{iV2})=0$. To overcome this drawback, it is possible to employ two non-orthogonal incident polarization states, for example where one source is in a horizontal polarization state and the other source is in a 45° polarization state.

In the circuit **71**, the interference signals measured by the photodiodes **61** and **62** are bandpass filtered with central frequencies of 4.2 KHz and 4.7 KHz and a bandwidth of 10 Hz, in order to extract the interference components of each light source. In this regard, 4.2 KHz and 4.7 KHz are the harmonic frequencies of the interference signals H and V of the horizontal source **21** and the vertical source **22**, respectively. The interference components form the imaginary parts of the analytical signals $E_{x,y}(t)$, whose real parts are obtained through inverse Hilbert transformation:

$$Re\{E_{x,y}(t)\} = \frac{1}{\pi}P\int_{-\infty}^{\infty}\frac{Im\{E_{x,y}(\tau)\}}{\tau - t}\,d\tau, \tag{7}$$

where P stands for the Cauchy principal value of the integral, and x and y represent the detected polarization state (H or V) and the source polarization state (H or V), respectively.

Unlike other transforms, the Hilbert transformation does not change the domain. A convenient method of computing the Hilbert transform is by means of the Fourier transformation. If u(t) and v(t) are a Hilbert pair of functions, that is

$$u(t) \overset{H}{\Leftarrow\Rightarrow} v(t)$$

and U(w) and V(w) are the Fourier transforms of u(t) and v(t), the following can be used to calculate the Hilbert transform:

$$\begin{aligned} &u(t) \overset{F}{\Rightarrow} U(w) \Rightarrow V(w) = -i\cdot sgn(w)U(w) \overset{F^{-1}}{\Longrightarrow} v(t) \\ &v(t) \overset{F}{\Rightarrow} V(w) \Rightarrow U(w) = i\cdot sgn(w)U(w) \overset{F^{-1}}{\Longrightarrow} u(t), \end{aligned} \tag{8}$$

where F and F^{-1} denote the Fourier and inverse Fourier transformations, respectively; and sgn(w) is the signum function defined as

$$sgn(w) = \begin{cases} +1 & w > 0 \\ 0 & w = 0\,. \\ -1 & w < 0 \end{cases}$$

The real and imaginary parts of each interference component are combined to form the complex components of the output Jones vectors. Upon determining the output Jones vector, when the input Jones vectors are known, the elements of the Jones matrix J of the sample can then be calculated from Equation (6).

The apparatus **10** of FIG. **1** was subjected to some initial testing, which involved measuring the matrix of a quarter wave plate at various orientations in combination with a mirror. The upper and lower portions of FIG. **2** are two related graphs. The graph in the upper portion of FIG. **2** shows the amplitude of the vertical components of the measured Jones vector versus the orientation of the quarter wave plate, where the amplitude of each Jones vector was normalized to unity. The graph in the lower portion of FIG. **2** shows the phase differences between the vertical components and the horizontal components of the Jones vectors. The results were calculated by averaging more than 1000 points centered at the peak of the interference signals, where adjacent points have a spacing which corresponds to a 10-μm resolution of the system. The graphs in FIG. **2** show that the measured data agrees very well with the theoretical data.

After verifying the operational characteristics of the apparatus **10** with these initial tests, the apparatus **10** was used to image an actual sample of soft tissue. In particular, a piece of porcine tendon was mounted in a cuvette filled with saline solution. The sample was transversely scanned with a step size of 5 μm through movement of the table **16** in a direction parallel to the arrow **17**, and multiple A-scan images were taken.

The interference signals were first band-pass filtered and Hilbert transformed in the manner discussed above, in order to extract the analytical signals of each polarization component. The analytical signals were then demodulated. For each A scan, pixels were formed by averaging the calculated elements of the Jones matrix over segments of 1000 points. Two-dimensional (2D) images were formed from these A-scan images, and were then median filtered. Then, each 2D Mueller-matrix image was pixel-wise normalized with an M_{00} image. The resulting 2D images are shown in FIG. **3**. In this discussion, each reference which is in the form M_{XY} represents a reference to the image appearing in row X and column Y of FIG. **3**. In FIG. **3**, each image corresponds to a size of 0.5 mm by 1.0 mm.

Clear band structures can be seen in some of the images, especially in M_{13}, M_{22}, M_{23}, M_{31}, M_{32}, and M_{33}. There is no such band structure present in the M_{00} image, which is the image based on the intensity of the back-scattered light. In other words, the M_{00} image is free of the effect of polarization. It is believed that the band structure is generated by the birefringence of the collagen fibers in the porcine tendon. The band structure distributes quite uniformly in the measured region. Therefore, the birefringence is also uniform in the measured area.

The foregoing discussion has been directed to a technique for efficiently acquiring a Mueller matrix of a sample. However, acquisition of the Mueller matrix of a sample is only a first step. Once the Mueller matrix has been obtained, it can be decomposed in order to extract significant information regarding the optical polarization properties of the sample, such as retardation, orientation of the major axes, and diattenuation. The polarization properties may be correlated to the normal or abnormal condition of biological tissue.

A non-depolarizing Mueller matrix can be decomposed by polar decomposition:

$$M=M_P M_R,\ \text{or}\ M=M'_R M'_P, \tag{9}$$

where M_P and M'_P are the Mueller matrices of a diattenuator (partial polarizer), and M_R and M'_R are the Mueller matrices of an elliptical retarder. To verify the decomposition, polarization information was extracted from a piece of porcine tendon at various orientations. If only linear diattenuation is considered, elements M_{31} and M_{32} in Equation (4) become:

$$M_{31}=P_1P_2\sin(2\theta)\sin(\delta),\ \text{and}\ M_{32}=-P_1P_2\cos(2\theta)\sin(\delta), \tag{10}$$

where P_1, P_2 are the principal coefficients of the amplitude transmission for the two orthogonal polarization eigenstates of the partial polarizer; θ is the orientation of the fast axis of the retarder; and δ is the phase retardation of the retarder. The calculated 2D images of M_{31} and M_{32} were averaged over segments of twenty A scans, and were fitted for a physical depth of 0.4 mm from the surface, assuming that the sample has a refractive index of n=1.4. The calculated retardation from the fitted data is $(4.2\pm0.3)\times10^{-3}$, which is comparable to a known value of (3.7±0.4)x10−3 for bovine tendon. The calculated angles of the fast axis for tissue fiber orientations varying with an interval of 10° are (0±4)°, (9±2.9)°, (20.9±1.9)°, (30±2.8)° and (38±4.3)° after subtracting an offset angle. The small angular offset is due to the discrepancy between the actual and the observed fiber orientations. The results were very good, considering that the tendon was slightly deformed when it was mounted in the cuvette, and the center of rotation for the sample may not have been exactly collinear with the optical axis. The diattenuation, defined as

$$D=(P_1^2-P_2^2)/(P_1^2+P_2^2)=\sqrt{M_{01}^2+M_{02}^2+M_{03}^2}\Big/M_{00},$$

was averaged over all of the orientations, and linearly fitted over a depth of 0.3 mm. The fitted diattenuation D versus the round-trip physical path length increased with a slope of 0.26/mm, and reached 0.075±0.024 at a depth of 0.3 mm, after subtracting an offset at the surface.

Alternative Embodiments

FIG. **4** is a block diagram of an apparatus **101** which is an alternative embodiment of the apparatus **10** of FIG. **1**. The apparatus **101** of FIG. **4** differs from the apparatus **10** of FIG. **1** primarily in regard to the configuration of the source arm, or in other words the portion of the apparatus to the left of the non-polarizing beam splitter **18**. Parts in FIG. **4** which are equivalent to parts in FIG. **1** are identified with the same reference numerals.

The apparatus **101** includes a superluminescent diode **103**, which is equivalent to either of the diodes **21** or **22** of FIG. **1**. The radiation emitted by the diode **103** is polarized, and travels to a non-polarizing beam splitter **106**. The splitter **106** splits the beam from the diode **103** into two separate beams of equal intensity, one of which then passes through an acousto-optical modulator (AOM) **107** of a known type, and the other of which is reflected by a mirror **111** and then passes through a half wave plate **112** and a modulator **113**. The plate **112** is oriented at 45°, and converts the beam into its orthogonal polarization state. The modulators **107** and **113** modulate the two beams at different frequencies, which are respectively 3 KHz and 3.5 KHz.

The modulated beam from the modulator **107** travels to the polarizing beam splitter **26**, and the modulated beam from the modulator **113** is reflected by a mirror **114** and then travels to the splitter **26**. The splitter **26** merges the two modulated beams in the manner discussed above in associated with FIG. **1**. The remaining portion of FIG. **4** is generally similar to the corresponding portion of FIG. **1**, and is therefore not described here in detail.

As evident from FIG. **4**, one of the two beams from the splitter **106** follows a longer path than the other beam in order to reach the splitter **26**. The difference between the lengths of these two paths is much longer than the coherence length of the optical beam from the diode **103**. Consequently, when the splitter **26** combines the component beams, the resulting combined light beam is equivalent to a light beam merged from two independent light sources of difference modulation frequencies with orthogonal polarization states.

FIG. **5** is a block diagram of an apparatus **131** which is an alternative embodiment of a portion of the source arm in the apparatus **101** of FIG. **4**. Equivalent parts are identified by the same reference numerals, and only the differences are discussed in detail. In particular, the half wave plate **112** of FIG. **4** is omitted in the apparatus of FIG. **5**, and the non-polarizing beam splitter **106** of FIG. **4** is replaced with a polarizing beam splitter **133**. The beam from the diode **103** is polarized at 45°, and is split by the splitter **133** into two beams having orthogonal polarization states. The remainder of the apparatus **131** is similar in structure and operation to the corresponding portion of the apparatus **101** of FIG. **4**.

FIG. **6** is a block diagram of an apparatus **151** which is yet another alternative embodiment of the apparatus **10** of FIG. **1**. Parts in FIG. **6** which are equivalent to parts in FIG. **1** are identified with the same reference numerals, and only significant differences are described here. The primary differences are in the configuration of the source arm, which as discussed above is the portion of the apparatus to the left of the splitter **18**.

The apparatus **151** includes a superluminescent diode **153**, which emits radiation that travels to an electrically controlled polarization rotator (EPR) **156**. The EPR **156** is a commercially available device of a known type. The EPR **156** is controlled by a controller **158**, which also controls the movement of tables **16** and **41**. The controller **158** causes the EPR **156** to alternately switch in a cyclic manner between two different operational modes. In one operational mode, the radiation from diode **153** which is passing through the EPR **156** is given a first polarization state, and in the other mode the radiation from diode **153** is given a second polarization state orthogonal to the first polarization state. In other words, this is a time division or time sharing approach, in which the photodiodes **61** and **62** are alternately operated to detect information for respective polarization states in successive alternating time slots, rather than being operated simultaneously as in the embodiment of FIG. **1**.

FIG. **7** is a block diagram of an apparatus **201** which is still another alternative embodiment of the apparatus **10** of FIG. **1**. Equivalent parts are identified with the same reference numerals, and only the differences are described below. The source arm to the left of the splitter **18** is similar to the source arm in FIG. **1**, except that a half wave plate **203** is provided between the filter **27** and the splitter **18**. As discussed earlier, the diodes **21** and **22** are modulated at different frequencies. When the two source beams from these diodes reach the half wave plate **203**, they are converted into +45° (P) and −45° (M) polarization states.

In the reference arm, a table **206** is supported for linear reciprocal movement in directions indicated by a double-headed arrow **207**. A polarizing beam splitter **208** is supported on the table **206**. The table **206** also supports a piezoelectric transducer (PZT) **213** and a piezoelectric transducer **214**, each of which movably supports a respective mirror **211** or **212**. A lens **216** is disposed between the splitter **208** and mirror **211**, and a lens **217** is disposed between the splitter **208** and mirror **212**. The transducers **213** and **214** are driven with signals having different frequencies, so that the transducers effect vibration of the mirrors **211** and **212** at different frequencies.

The two beam components which travel into the reference arm from the splitter **18** are each split by the splitter **208** into two subcomponents, which each pass through a respective lens **216** or **217**, and are each reflected by a respective mirror **211** or **212**. The reflected subcomponents then pass back through the respective lenses **216** and **217**, and are combined by the splitter **208**. The resulting beam is returned to the splitter **18**. Since the mirrors **211** and **212** are vibrated at different frequencies, they introduce different modulation frequencies into the horizontal and vertical polarization states represented by the respective subcomponents. As a result, the detection arm of the apparatus **201** needs only a single photodiode **221** to effect detection for the two orthogonal polarization components, rather than two separate photodiodes such as those shown at **61** and **62** in FIG. **1**. The reference arm includes an objective lens **222**, which directs radiation received from the splitter **18** into one end of a single-mode optical fiber **223**. The opposite end of the fiber **223** is connected to the photodiode **221**.

FIG. **8** is a block diagram of an apparatus **251** which is an alternative embodiment of the apparatus **101** shown in FIG. **4**. Equivalent parts are identified with the same reference numerals, and only significant differences are described in detail below. In the sample arm, radiation from the splitter **18** passes through an objective lens **256**, which directs the radiation into one end of a single-mode optical fiber **257**. A hand-held probe (HP) **258** is provided at the other end of the fiber **257**, and serves as an imaging head.

FIG. **9** is a diagrammatic sectional side view of the hand-held probe **258**. The end of the fiber **257** is coupled by a connector **259** to a fiber collimator, through which a beam of radiation enters the probe **258**. The probe has a motor **261** powered by a not-illustrated source, which can effect limited reciprocal pivotal movement of a mirror **262**. A lens **263** and a window **264** are supported on a housing of the probe **258**. The beam from the collimator **260** is reflected by the mirror **262**, and passes through the lens **263** and the window **264** to the sample **12** (FIG. **8**). Radiation reflected from the sample **12** travels back through the window **264** and lens **263**, is reflected again by the mirror **262**, and then travels back through the collimator **260** and into the fiber **257**. The movement of the mirror **262** by the motor **261** causes the beam impinging on the sample **12** to be linearly scanned across the sample.

Radiation which travels into the reference arm from the splitter **18** passes through a linear polarizer (LP) **266** oriented at 45°. This radiation then passes through a lens **267**, which directs it into a single-mode optical fiber **268**. When the radiation emerges from the opposite end of the fiber **268**, it passes through a lens **269**, and then through the lens **37** on the movable table **41**. This radiation is then reflected by the mirror **38**, and travels back through the lens **37**, lens **269**, fiber **268**, lens **267** and linear polarizer **266** to the splitter **18**.

FIG. **10** is a block diagram of an alternative embodiment of part of the apparatus of FIG. **1** and, in particular, is an alternative embodiment of part of the source arm of FIG. **1**. The apparatus **301** would be utilized in a situation where the sample **12** (FIG. **1**) does not happen to alter the polarization state of the light impinging on it, such that an orthogonal incident polarization arrangement of the type discussed above would not provide accurate phase information for the backscattered light. The apparatus **301** therefore uses polarization states for the two incident beams which are non-orthogonal, in that one is vertically polarized and the other is polarized at ±45°.

More specifically, the apparatus **301** includes two superluminescent diodes **303** and **304**. The beam from the diode **303** is polarized at 45° by a polarization plate (PP) **306**, and the beam from the diode **304** is vertically polarized by a vertical polarization (VP) plate **308**. The beams from the plates **306** and **308** are each supplied to a non-polarizing beam splitter **307**, which combines these beams. The resulting beam is then supplied to a spatial filter of the type shown at **27** in FIG. **1**.

FIG. **11** is a block diagram of an apparatus **351** which is an alternative embodiment of the apparatus **301** of FIG. **10**. Equivalent parts are identified by the same referenced numerals. The primary difference is that the polarizing plate **306** of FIG. **10** is replaced with a circular polarization plate **353**, which is a one-eighth wave plate oriented at 22.5°. The plates **353** and **308** respectively give the two beams circular and vertical polarizations.

Advantages

The present invention provides a number of technical advantages. One such advantage is that, when using polarization-sensitive OCT imaging, Mueller matrix images of an object can be obtained with a single scan. On a more specific level, the Jones matrix of the sample is determined during the single scan, and then the Jones matrix is transformed into an equivalent Mueller matrix. This facilitates the acquisition of two-dimensional tomographic Mueller-matrix images of an unstable sample such as biological tissue, either in vivo or in vitro. A further advantage is that the image information has relatively high spatial resolution. Yet another advantage is that the Mueller matrix can be decomposed in order to extract information on optical polarization properties of the sample, such as retardation, orientation of the major axes, and diattenuation. The polarization properties may be correlated to normal or abnormal conditions of biological tissues.

Although several selected embodiments have been illustrated and described in detail, it should be understood that various substitutions and alterations are possible without departing from the spirit and scope of the present invention, as defined by the following claims.

What is claimed is:

1. A method, comprising the steps of:

causing an object to emit polarized radiation by:

- transmitting predetermined radiation to said object;
- generating first and second optical beams having different polarizations; and
- splitting each of said first and second beams into first and second components, said first components each being directed to said object to cause said object to emit said polarized radiation;

directing each of said second components to a reference section where each said second component is reflected by a reflective surface which is physically modulated to thereby generate modulated components;

forming further radiation from said modulated components and said polarized radiation;

detecting said polarized radiation comprising said further radiation;

determining a Jones matrix based on information obtained in said detecting step from said polarized radiation; and

transforming said Jones matrix into a Mueller matrix, said Mueller matrix being representative of properties of said object.

2. A method according to claim **1**, including the step of decomposing said Mueller matrix to obtain information representative of optical polarization properties of said object.

3. A method according to claim **1**, including the step of selecting an unstable material as said object.

4. A method according to claim **3**, wherein said step of selecting said unstable material includes the step of selecting biological tissue as said object.

5. A method according to claim **1**, wherein said step of causing said object to emit polarized radiation involves polarization-sensitive optical coherence tomography.

6. A method according to claim **1**,

wherein said transmitting step includes the step of scanning said predetermined radiation physically across said object; and

wherein said Jones matrix is determined from information obtained in said detecting step during a single said scan.

7. A method according to claim **1**, including the step of selecting optical radiation as said predetermined radiation, said polarized radiation being optical radiation.

8. A method according to claim **7**, wherein said predetermined radiation includes first and second portions which have different polarizations.

9. A method according to claim **1**, wherein said step of generating said first and second optical beams is carried out by generating said first and second optical beams successively in time.

10. A method according to claim **1**, wherein said step of generating said first and second optical beams is carried out by simultaneously generating said first and second optical beams.

11. A method according to claim **1**, including the steps of:

providing first and second detectors; and

splitting said further radiation into two components which are each routed to a respective one of said detectors.

12. A method according to claim **11**, including the step of configuring said reference section so that each said second component is reflected by the same reflective surface.

13. A method according to claim **1**, including the steps of:

configuring said reference section to have two of said reflective surfaces which are physically modulated at different frequencies, each of said second components being reflected by a respective one of said reflective surfaces; and

routing said further radiation to one detector which effects said detecting step.

14. A method according to claim **1**, including the steps of:

providing a first optical fiber, said first components and said polarized radiation traveling through said first optical fiber in respective directions which are opposite; and

configuring said reference section to include a second optical fiber, said second components and said modulated components traveling through said second optical fiber in respective directions which are opposite.

15. An apparatus, comprising:

a first section operable to detect polarized radiation emitted by an object;

a second section operable to determine a Jones matrix based on information obtained by said first section from said polarized radiation, and to thereafter transforms said Jones matrix into a Mueller matrix, said Mueller matrix being representative of properties of the object; and

a third section operable to transmit to the object predetermined radiation which causes the object to emit said polarized radiation, said third section comprising:

- a source section which generates first and second optical beams having different polarizations;
- a splitter which splits each of said first and second beams into first and second components;
- a sample section which directs said first components to the object to cause the object to emit said polarized radiation and which directs said polarized radiation from the object to said splitter; and
- a reference section which is operable to cause each said second component to be reflected by a reflective surface which is physically modulated to thereby generate modulated components;
- wherein said splitter is operable to form further radiation from said modulated components and said polarized radiation, said first section being responsive to said further radiation.

16. An apparatus according to claim **15**, wherein said second section is operable to decompose said Mueller matrix to obtain information representative of optical polarization properties of the object.

17. An apparatus according to claim **15**,

wherein said third section is operable to scan said predetermined radiation physically across the object; and

wherein second section is operable to effect said determination of said Jones matrix from information obtained during a single said scan.

18. An apparatus according to claim **15**, wherein said predetermined radiation is optical radiation, and said polarized radiation is optical radiation.

19. An apparatus according to claim **18**, wherein said predetermined radiation includes first and second portions which have different polarizations.

20. An apparatus according to claim **15**, wherein said source section generates said first and second optical beams successively in time.

21. An apparatus according to claim **15**, wherein said source section generates said first and second optical beams simultaneously.

22. An apparatus according to claim **15**,

wherein said first section includes first and second detectors; and

including a splitter which splits said further radiation into two components that are each routed to a respective one of said detectors.

23. An apparatus according to claim **22**, wherein said reference section effects said reflection of each of said second components using the same reflective surface.

24. An apparatus according to claim **15**,

wherein said reference section includes two of said reflective surfaces which are physically modulated at different frequencies, each of said second components being reflected by a respective one of said reflective surfaces; and

wherein said first section includes one detector which effects said detection of said polarized radiation.

25. An apparatus according to claim **15**,

wherein said sample section includes a first optical fiber, said first components and said polarized radiation traveling through said first optical fiber in respective directions which are opposite; and

wherein said reference section includes a second optical fiber, said second components and said modulated components traveling through said second optical fiber in respective directions which are opposite.

26. An apparatus according to claim **25**, including at an end of said first optical fiber remote from said splitter a hand-held probe which can be manually moved relative to the object.

27. An apparatus according to claim **26**, wherein said hand-held probe includes structure operable to effect a scanning movement of a direction in which said first components are emitted from said probe.

* * * * *